Desalination and Water Treatment
www.deswater.com
doi: 10.5004/dwt.2022.28015

257 (2022) 169–184
May

Application of response surface methodology for modelling of direct contact membrane distillation system: a review

Siti Nurina Adlina Binti Roslan[a], Nur Hashimah Alias[a,*], Nur Hidayati Othman[a], Mohd Haiqal Abd Aziz[b], Fauziah Marpani[a], Muhammad Shafiq Mat-Shayuti[a], Munawar Zaman Shahruddin[a], Tutuk DjokoKusworo[c]

[a]*Department of Oil and Gas Engineering, School of Chemical Engineering, College of Engineering, Universiti Teknologi MARA, 40450 Shah Alam, Selangor, Malaysia, emails: nurhashimah@uitm.edu.my (N.H. Alias), adlinanurieyna98@gmail.com (S.N. Adlina Binti Roslan), nurhidayati0955@uitm.edu.my (N.H. Othman), fauziah176@uitm.edu.my (F. Marpani), mshafiq5779@uitm.edu.my (M.S. Mat-Shayuti), munawar_zaman@uitm.edu.my (M.Z. Shahruddin)*
[b]*Department of Chemical Engineering Technology, Faculty of Engineering Technology, Universiti Tun Hussein Onn Malaysia, Pagoh Higher Education Hub Muar, 84600 Johor, Malaysia, email: haiqalabdaziz@gmail.com*
[c]*Department of Chemical Engineering, Faculty of Engineering, Diponegoro University, Semarang 50275, Indonesia, email: tdkusworo@che.undip.ac.id*

Received 21 September 2021; Accepted 28 November 2021

ABSTRACT

This paper discusses the response surface methodology (RSM) study on a recent direct contact membrane distillation (DCMD) system. The DCMD system is reviewed due to its myriad attention on desalination process, especially on water treatment of high salinity and reclamation of industrial process water. The fundamental of DCMD, as well as the mass and heat transfer principles for modelling the system, are firstly explained and compared with previous studies. Then, the researcher highlighted the parameters involved in the modelling of DCMD process, such as feed temperature, velocity, and concentration, simultaneously with common membrane properties in mass and heat transfer models. The correlation of these frequently studied parameters with the conventional model was included and summarised. Subsequently, RSM was performed for the model development of the DCMD system, which included common design matrix applications, such as Box–Behnken, central composite design, and full factorial design. Finally, this work reviews the most recent application for the DCMD modelling of the model, comparing its experimental number runs, independent input number, model levels, and accuracy for optimising the DCMD process using RSM.

Keywords: Response surface methodology; Membrane distillation; Desalination; Direct contact membrane distillation; Modelling

1. Introduction

The increase in population, climate change, and pollution have all contributed to freshwater scarcity. As such, the use of seawater desalination as a sustainable source of drinking water is seen as a solution to address the aforementioned issue. Desalination using membrane distillation is an emerging alternative to the conventional reverse osmosis (RO) process in saline water treatment [1]. To date, RO has been widely used in industrial plants for commercial-scale desalination processes, which cover nearly 69% of the world's saline water [2,3]. This is attributed to the main advantages of RO, which include high salt rejection and high permeation. Despite its benefits, the RO process

* Corresponding author.

Presented at the 5th International Conference on Global Sustainability and Chemical Engineering (ICGSCE 2021), 14–15 September 2021, Virtual Conference organized by Universiti Teknologi Mara (UiTM), Selangor, Malaysia

1944-3994/1944-3986

consumes nearly 4 kWh/m^3 of electricity for its system, requires high pressure (5.5–6.8 MPa), and has limitations with high salinity feed [4–6]. As a result, there is a growing interest in membrane distillation-based desalination as a potential alternative to provide nearly 100% rejection of non-volatile compounds at moderate operating conditions [7]. Membrane distillation (MD) technology is known to be highly efficient, with lower energy consumption when compared with RO, as well as its versatility and technological capacity, which allows the process to treat a wider range of water and wastewater [8]. The current effort to improve MD technology includes ease of operation, less chemical usage, and low energy consumption, leading to its growing acceptance in the industry [9,10].

However, these processes are still subject to a variety of constraints, such as temperature polarisation and fouling issues, which result in lower desalination performance [11–13]. The temperature polarisation often led to a decrease in flux rejection in the MD process. Thus, this situation necessitates an optimisation solution, which can be achieved by employing various modelling approaches, such as conventional mass and heat transfer modelling, computational fluid dynamics (CFD), and response surface methodology (RSM). The conventional method of system optimisation requires numerous time-consuming experiments, whereby this limitation is portrayed by the conventional method, thus highlighting the importance of RSM implementation in order to save time and cost through reduced number of trials [14].

The MD process is commonly operated at low feed temperatures ranging from 50°C to 80°C at atmospheric pressure. In MD, the heated liquid feed/seawater is commonly brought into contact with the membrane, with the cold-water stream flowing on the other side of the membrane (permeate side) [15]. The driving force for this process is attributed to the temperature difference between the permeate and feed stream, which creates a vapour pressure gradient that moves the water molecule across hydrophobic membrane [15]. The evaporated water molecule is further condensed at the other side of the membrane (permeate side), resulting in a very pure drinkable water. Therefore, the MD process is observed to have included both mass and heat transfer in order to successfully drive pure water fluxes, leaving contaminants from the feed liquids, as illustrated in Fig. 1.

Membrane distillation is generally classified into four types: direct contact membrane distillation (DCMD), vacuum membrane distillation (VMD), sweeping gas membrane distillation and air-gap membrane distillation [16,17]. Among the numerous approaches to conducting membrane distillation processes each has advantages and disadvantages. However, this paper focuses on the DCMD type of configuration because it is the most commonly used and studied MD configuration due to its simplicity, as well as its ability to reject all dissolved non-volatile species in water [15,18,19]. For instance, when compared with the VMD, as shown in Figs. 2 and 3, the DCMD's operation at atmospheric pressure and ability to treat a saline feed with various concentrations while eliminating the need for an additional external condenser make DCMD an appealing system to further study and optimise [20,21]. Though there is a requirement for the feed/permeate pump to provide adequate turbulence in mitigating the concentration and temperature polarisation issues commonly associated with the MD system [22], the pumps used in the DCMD process can be fabricated with low-cost plastics due to the low pressure operation [10]. Despite these advantages, industrial commercialisation of DCMD remains limited due to a variety of technical issues, most notably material efficiency, module design, and maintenance cost [23,24]. The need for external energy supply can be substituted by using solar panels, as shown in the study by Bamasag et al. [25] and Lee et al. [26]. Furthermore, the application of this solar panel has been studied by Soomro and Kim for the 111-MWe SPT plants integrated with the DCMD system in Abu Dhabi, United Arab Emirates, as specified in Fig. 4. The study results in a low-cost value for energy and water production per meter,

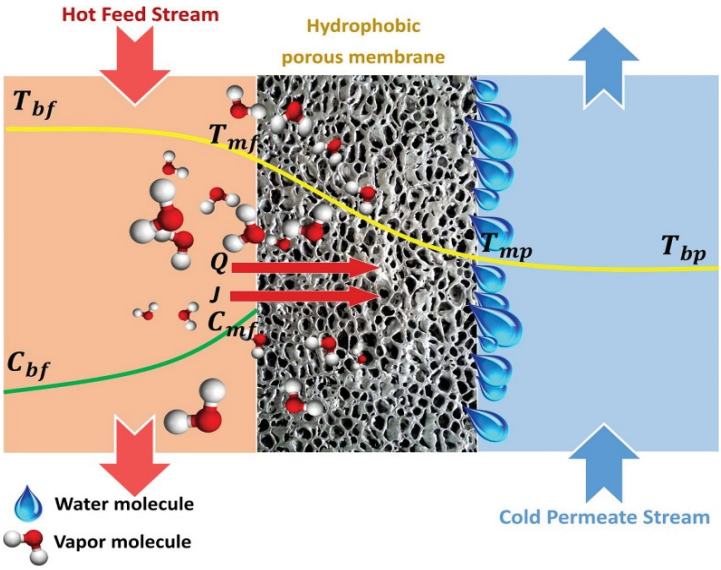

Fig. 1. Schematic representation of heat and mass transfer across the membrane in the DCMD system [15].

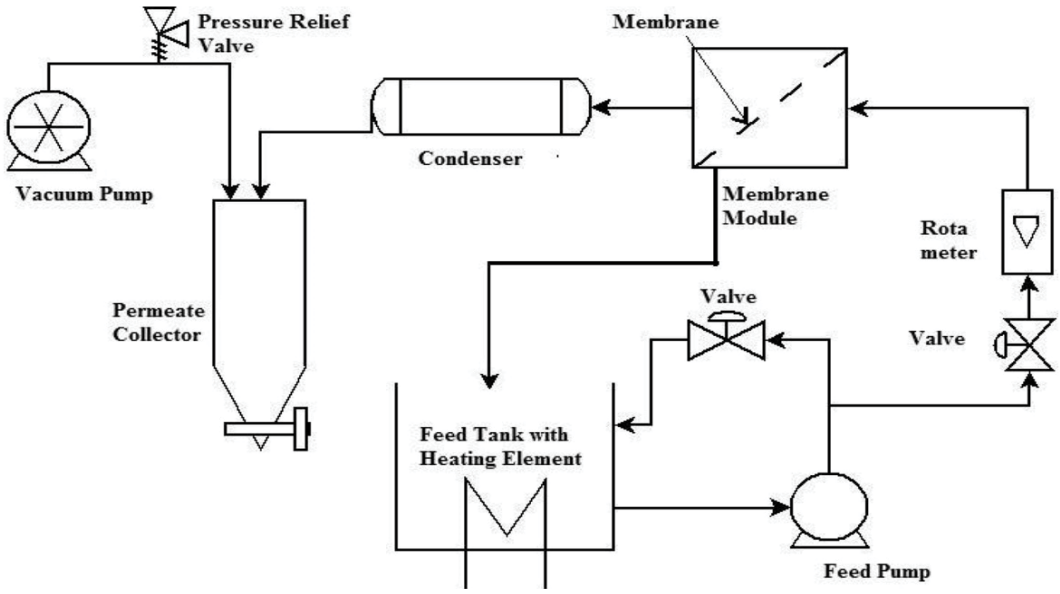

Fig. 2. Schematic diagram of VMD operation [28].

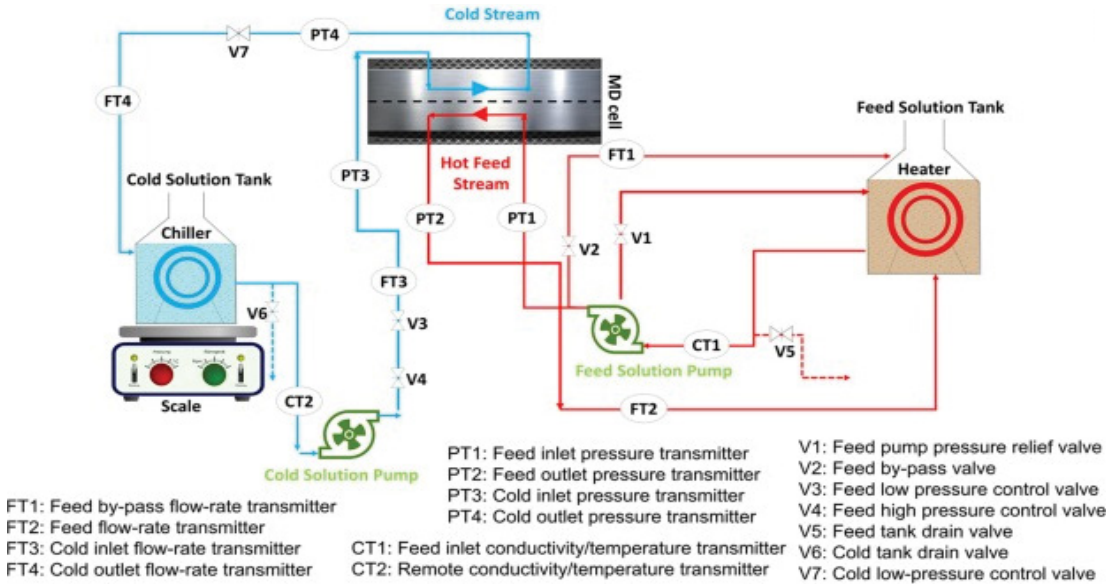

Fig. 3. Schematic diagram of DCMD operation [15].

indicating that the system is economically feasible. Its implementation would significantly overcome the freshwater crisis and electricity unavailability globally [27].

2. Fundamental of DCMD

In DCMD configuration, the heat and mass transfer follow the basic MD principle. Fig. 5 shows the DCMD schematic diagram with temperature variation along hydrophobic membrane with the hot solution (feed) is in direct contact with one side of the membrane surface. The hot solution (feed) is in direct contact with one side of the membrane surface. Evaporation occurs on the feed side, and water vapour movement into the membrane (gas phase only) towards the permeate side is caused by the pressure difference between the hot feed and the permeate stream [29,30]. Water vapour condenses into water droplets in the permeate stream once it reaches the cold-permeate side of the membrane. Because the configuration involves direct contact between the membrane surface and the permeate liquid phase, heat is quickly transferred from the feed side into the permeate stream, favouring temperature polarisation. This significant temperature difference may result in heat conduction loss, thereby possibly reducing the overall thermal efficiency. Notably, the temperature difference has had a significantly impacted on the efficiency of membrane distillation [31]. In recent years, a number of studies involving the modification of DCMD have been conducted, involving both the

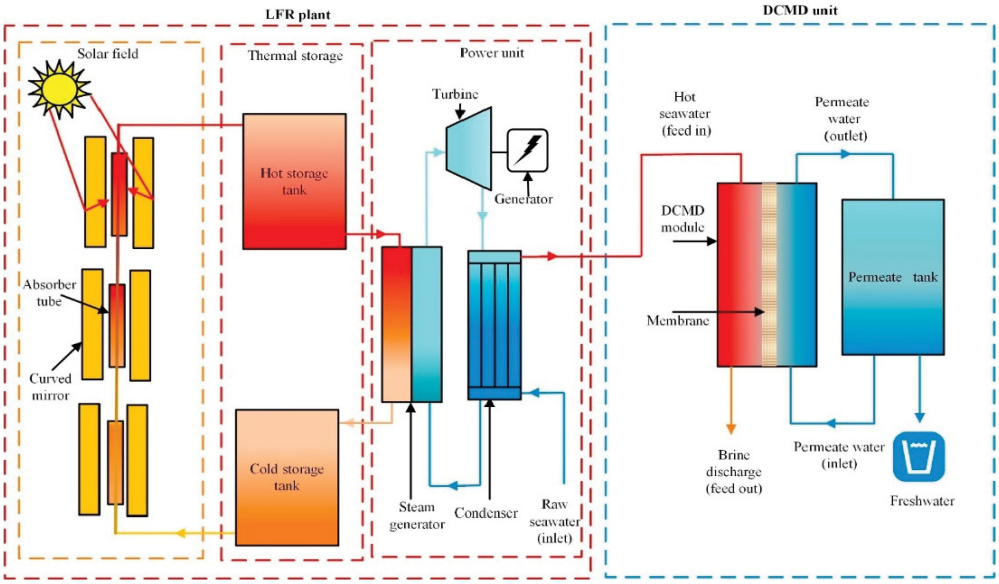

Fig. 4. Schematic diagram of Linear Fresnel Reflector plant integrated with DCMD system [27].

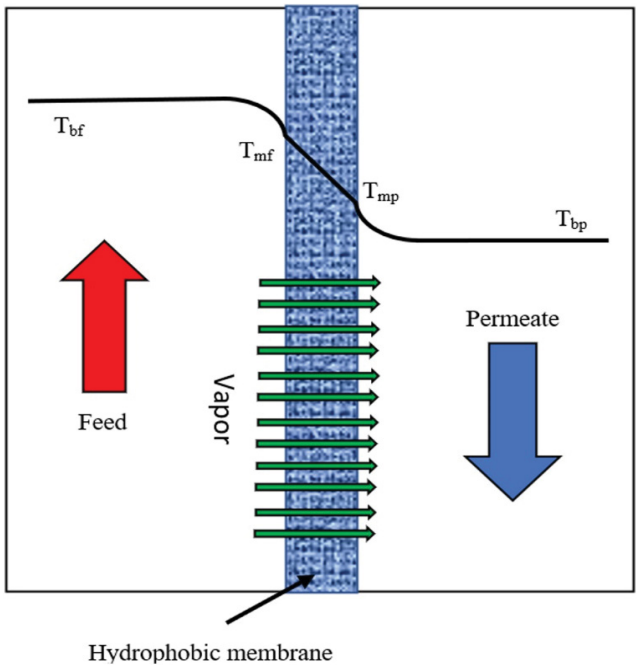

Fig. 5. DCMD diagram with temperature variation along hydrophobic membrane [37].

operating conditions and membrane properties modification, such as in the [32–36] study with the various objective/input parameters being studied. Optimisation is required to obtain the most efficient condition or highest quality of fabricated membrane for DCMD application. Table 4 summarises numerous studies that have implemented a design matrix for RSM application, which show deviations in the range of 0.5%–5% deviations. The optimisation predicts the best operating condition for the DCMD process, with a slight deviation from the experimental data. The following section discusses the DCMD processes that are modelled using conventional mass and heat transfer and RSM.

3. Model for DCMD

This section discusses the appropriate model (i.e., mass and heat transfer model) and RSM for the DCMD process based on a literature search.

3.1. Mass and heat transfer model

Mass transfer in the DCMD unit acquires the permeate solution temperature lower than the feed solution, forcing the vapour molecule transfer through the membrane pores and condensation at the permeate side [38]. When the feed solution reaches the evaporation limit, vapour is formed at the membrane boundary layer, and the mass transfer begins. It can be seen that mass transfer across the membrane is primarily determined by the difference in vapour partial pressure between the two sides of the membrane, as shown in Eq. (1):

$$J(T) = B(T)\left(P_{mf}(T) - P_{mp}(T)\right) \tag{1}$$

where $J(T)$ is the permeate flux (kg/m^2 s); and $P_{mf}(T)$ and $P_{mp}(T)$ are the interfacial pressure along membrane boundaries between feed solution and permeate solution, respectively. In most cases, the flow pattern in the membrane is a mix of Knudsen diffusion and ordinary molecular diffusion [39]. The membrane mass transfer coefficient, $B(T)$, of the process can be expressed in Eq. (2):

$$B(T) = \frac{1}{\left(\frac{\tau\delta}{\varepsilon}\frac{P_a}{PD}\frac{RT}{M} + \frac{3}{2}\frac{\tau\delta}{\varepsilon r}\left(\frac{8M}{\pi RT}\right)\right)^{-1/2}} \tag{2}$$

where ε, r, τ and δ are the porosity, tortuosity, pore radius, and membrane thickness, while P is the total pressure inside the pore, and D is the water diffusion coefficient. P_{mf}/P_{mp} are partial water vapour pressure on feed or permeate sides, respectively, which can be calculated by using Eqs. (3) and (4) [39]:

$$P_{mf/mp} = (1-x)\left(1-0.5x-10x^2\right)P^v \tag{3}$$

The P^v in the equation above is the water vapour pressure, while x is the salt molar fraction in either feed or permeate sides. Thus, the P^v can be calculated according to Eq. (4), where T in the equation represents the solution temperature.

$$P^v = \exp\left(23.1964 - \frac{3{,}816.44}{T-46.13}\right) \tag{4}$$

The heat transfer model in the membrane distillation process is generally described and quantified based on the heat transfer occurring in the membrane by predicting the membrane interface temperature [18]. Some of the parameter values generated by the heat transfer model are essential to complete the mass transfer model. The combination of both of these models allows the output, which is often water flux, to be predicted. The heat transfer model is divided into four different parts based on the region of the membrane; heat transfer from the feed bulk to the membrane interface, heat flux through the membrane, heat transfer due to evaporated water flux, and heat transfer from the permeate membrane interface to the bulk of the permeate side [18,40]. Moreover, it is noteworthy that in an equilibrated MD module, the heat flux in the water channel and membrane must be equal according to the conservation of energy and mass law in the thermodynamics [38], which applies to different regions in the DCMD process, as specified in Fig. 6.

The total heat transferred from the feed solution through the membrane and permeate sides are calculated using Eqs. (5) and (6). The K_m is the average membrane thermal conductivity; V_f and V_p are the convective heat transfer coefficient on feed and permeates solution, respectively; and A is the membrane area.

$$Q_f = AV_f\left(T_f - T_{mf}\right) \tag{5}$$

$$Q_p = AV_p\left(T_{mp} - T_p\right) \tag{6}$$

$$Q_m = \frac{Ak_m}{\delta_m}\left(T_{mf} - T_{mp}\right) + AJ(T)H(T) \tag{7}$$

The $H(T)$ in Eq. (8) represents the latent heat of evaporation, which can be expressed as per Eq. (8):

$$H(T) = 2{,}500.8 - 2.36T + 0.0016T^2 - 0.00006T^3 \tag{8}$$

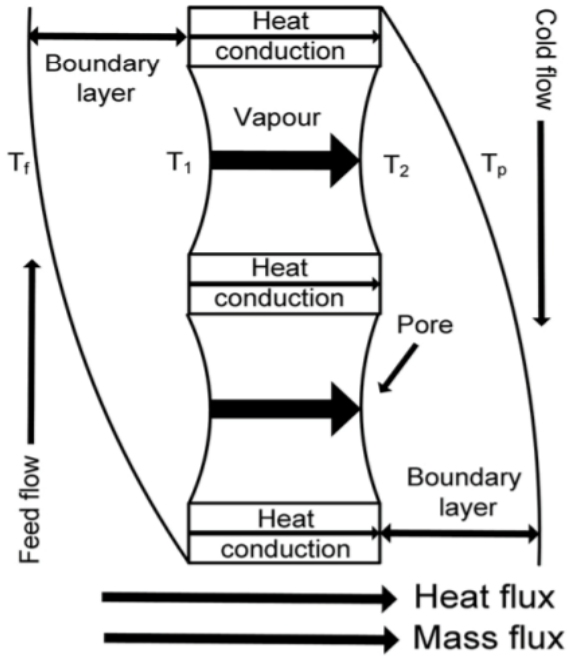

Fig. 6. Heat and mass transfer through the membrane [41].

The energy balance equation for the DCMD process can be concluded as in Eq. (9) [37,42]:

$$AV_f\left(T_f - T_{mf}\right) = \frac{Ak_m}{\delta_m}\left(T_{mf} - T_{mp}\right) + AJ(T)H(T) = AV_p\left(T_{mp} - T_p\right) \tag{9}$$

3.2. Response surface methodology model

Response surface methodology is an optimisation method that combines empirical statistical and mathematical techniques to model a specific system and provide quantitative analysis for the experimental, focusing primarily on the parameter to develop an optimised regression model [28,43]. Response surface methodology is implemented in a particular experiment by developing a linear or quadratic polynomial function that adjusts the output/response of the experiment based on the input parameter, such as operating conditions. The RSM can be designed using a variety of design methods, including Box–Behnken design, full factorial design (FFD), and central composite design (CCD), in which each has their own advantages and disadvantages [44]. However, a specific design method selection is normally dependent on the experimental points numbers for the number of variables and number of executions.

It is widely acknowledged that RSM has a few limitations, such as untrustworthy polynomials when extrapolated beyond the experimental region and intricate analysis when the number of experiments is too large. However, the benefits of using RSM outweigh the drawbacks of the traditional method. RSM is usually conducted with one factor at a time while keeping other factors constant, and is

favoured for optimisation compared with the conventional method. This conventional method serves to optimise the system but it is time-consuming and is high in experimental cost. Furthermore, conventional method implementation lacks in considering the interaction effect between different experimental parameters, which are achievable when RSM is used as the optimisation approach [28,45]. However, the researcher needs to sincerely acknowledge model development alongside the steps to conduct the RSM analysis, and they are further discussed in the next part of this paper.

3.2.1. Steps in conducting RSM

A few essential steps must be followed in order to successfully conduct RSM for optimisation, which include screening and analysis in order to select the primary input required to initiate the optimisation. Concurrently, the steps include eliminating any input variables that contribute less to the response [46]. The selection of input variables is important to decide the number of experiments to run for optimisation purposes. The next step is to choose the most suitable experiment design, such as Box–Behnken design, central composite design, or full factorial design, based on the experiment suitability. The suitability of the models is primarily determined by the experimental condition limits, which are highly dependent on the input parameters; this is further elaborated in Section 2.3. Following the selection of DOE, the number of experiments (N) is calculated with the specific DOE formula and is further specified in Section 2.3.1–Section 2.3.3. Generating the number of experiments allows the optimisation to be initiated using any suitable software for RSM, mainly Minitab and Design Expert. The regression equation, analysis of variance (ANOVA), and optimised points in the experiments were generated after the optimisation was performed using the software. The optimised points obtained from the optimisation model were validated by experimentation with the optimised parameter value [43,47]. However, if the optimisation points in the model generate highly deviated results, another model of the experimental equation and experimental design is preferred. Therefore, to finalise the RSM results, a graphical representation in three-dimensional (3D) surface modelling may be generated to facilitate studying the interactions between the various inputs and the response. The steps for conducting the RSM is summarised in Fig. 7.

3.2.2. Basis for model development

To understand the basis for the model development based on the design of the experiment method selected, it is essential to fully acknowledge the experimental parameter with its mathematical model, which measures the values of responses and the optimised results. Therefore, steps for screening and analysing input parameters in Section 2.2.1 is crucial in predicting the response parameter of interest (R) value. The R-value depends on the level of quantitative input variables X_1, X_2 … X_k and is expressed as [46]:

$$R = f\left(X_1, X_2, \ldots, X_k\right) \tag{10}$$

The relationship between the response parameter of interest (R) and the selected levels of quantitative input variables (X) can be either a linear or factorial model and can also be adjusted to second or third-order expression [46]. A first-order expression is implemented if the response can be defined with a linear function of an independent factor with the equation specified below.

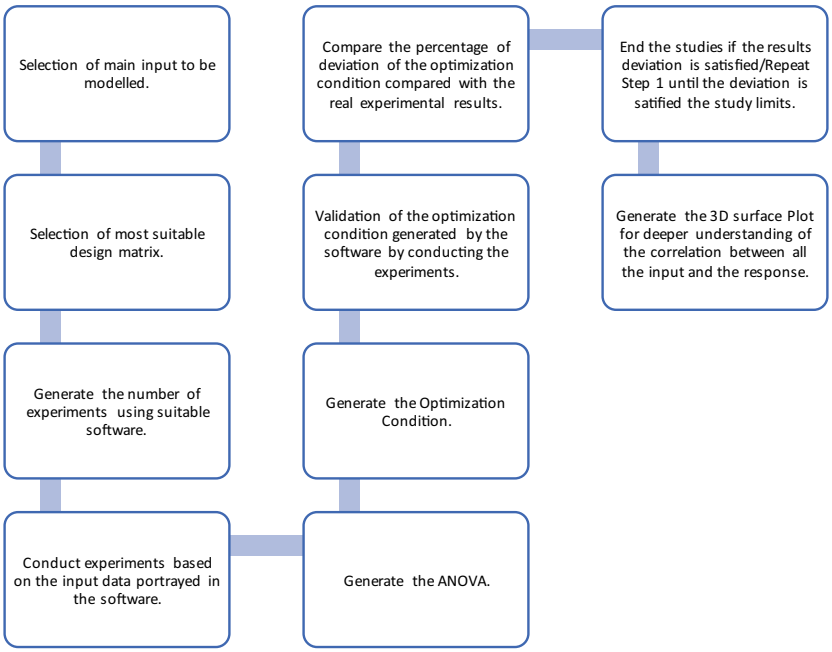

Fig. 7. Summary of steps to conduct RSM.

$$R = \beta_0 + \beta_1 X_1 + \beta_2 X_2 + \varepsilon \quad (11)$$

Meanwhile, the highly structured second-order expression model is expressed as:

$$R = \beta_0 + \beta_1 X_1 + \beta_2 X_2 + \beta_{11} X_{11}^2 + \beta_{12} X_{22}^2 + \beta_{12} X_1 X_2 + \varepsilon \quad (12)$$

In this equation, β_0 is the model constant; while β_1, β_2 are the model coefficients; X is the independent variables; k is the number of independent variables; and ε is a statistical error. The X_n in Eq. (12) represents the main effect for each input; X_1, X_n represent the interactions between the input factor; and X_n^n refers to the quadratic components for the input factor. The response surface can portray the relationship between response and level of factors. However, the level of each factor required is three for estimating the curvature of the response surface. The quadratic term is unable to be estimated if the centre point with two-level design is implemented adequately.

3.3. Types of common models

3.3.1. Box–Behnken design

Box–Behnken design (BBD) is one of the methods used in RSM experiment design. The BBD is an exciting model that allows the modelling of first and second-order response surface generation in contrast to three-level full factorial design, which requires three-levels for each input factor [48]. This advantage results in a more cost-effective modelling because of the fewer experimental runs required for the optimisation phase. The BBD offers response surface modelling without axial points and a significant number of continuous tests, with factors ranging from 3 to 7 [49]. Box–Behnken design requires three-levels per factor. However, to fit a second-order equation, twelve middle edge nodes and three centre nodes are required [50]. Fig. 8 shows that the Box–Behnken design acquires the points at the midpoints of cubical edges.

To obtain the number of experiments to be conducted using Box–Behnken design, Eq. (13) is applied:

$$N = 2\left(k\left(k-1\right)\right) + C \quad (13)$$

The k represents the number of input parameters of the same factor, while coefficient ($k(k-1)$) represents the constant that considers the min and max of other parameter levels. The coefficient C represents the centre points in the BBD.

3.3.2. Central composite design

The central composite design is one of the most implemented designs aside from the Box–Behnken design [19,28]. The central composite design of the experiment comprises a factorial design with a central point extended with a group of axial points [46]. The central composite design combines Box–Behnken design and Box–Wilson design comprising the points at the centre of the experiment domain and star points outside the domain, as shown in Fig. 9. There are three basic types of central composite designs, which are central composite face-centred (CCF), central composite circumscribed (CCC), and central composite inscribed (CCI). Table 1 summarises the difference between these various CCD methods.

These design types vary based on selecting experimental points, several variables, and executions [46]. For the CCF and CCI, the design can be run at 5 levels: +α, –α, central point, +1, –1 [52]. Few elements are crucial in determining the experimental points number of levels each for variables and its execution which are α-value, factor number (k), replicate number (C_p). α-value is the distance of each star points from the centre of CCD, where this value depending on the number of variables and can be calculated using Eq. (14).

$$\alpha = \left(2^k\right)^{0.25} \quad (14)$$

The α-value for a specific CCD model would indicate the axial point location outside or inside the cube, α-value less than 1 portrays the location of the axial point as a cubic shape, while for α-value greater than 1, the axial points located outside the cube [47]. The ability to acknowledge the α-value for a specific model would suggest the type for CCD design, whether it is CCF, CCI, or CCC. The number

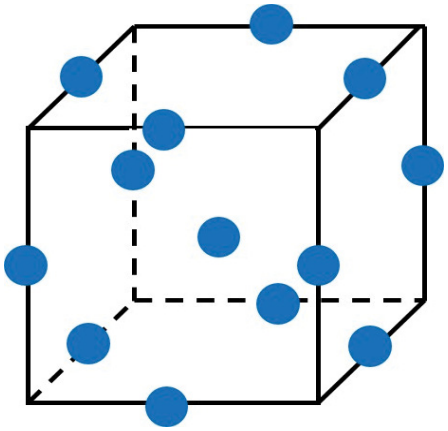

Fig. 8. Box–Behnken design matrix.

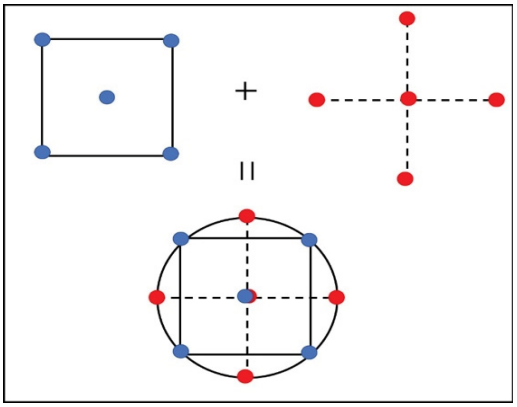

Fig. 9. Generation of central composite design.

Table 1
Difference between three types of central composite design [51]

Type of central composite design	Difference	Experimental
Central composite circumscribed (CCC)	Requires 5 level per factor. Star points are located outside of the initial experimental domain.	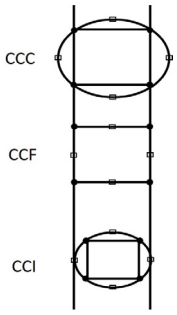
Composite face-centred (CCF)	Requires 3 level per factor. Star points are located on the experimental domain face.	
Central composite inscribed (CCI)	Requires 5 level per factor. Implemented if it is not possible to leave the experimental domain. The CCC are reduced to fit this domain.	

of the experiment is indicated in Eq. (15), where k is the factor number, and C_p is the central point replicate number [46,53].

$$N = k^2 + 2 \cdot k + C_p \tag{15}$$

3.3.3. Full factorial model

A full factorial model is a technique in modelling that enables the study of multiple independent variables with multiple levels for a dependent variable. This approach is used widely due to its efficiency in experimental runs, straightforward analysis, and ease in designing [54,55]. It is considered one of the effective methodologies in designing experiments that involve multiple factors with different outcomes value and involves design matrix with two levels of input parameters: lower bound and upper bound, which represents two levels for this design approach. The high and low combinations of low input factors are required to plan the experimental runs for both experiments and modelling. There are two known types of full factorial models. The two-level full factorial model is more suitable for the screening process, whilst the three-level full factorial model is more suitable for optimisation problems. The two-level full factorial model number of experimental trials is calculated in Eq. (16), where k represents the number of variables and L is the level of the variables. Fig. 10 illustrates a two-level full factorial design matrix illustration.

$$N = 2^k \tag{16}$$

Nevertheless, a two-level full factorial design is not suitable for optimisation purposes. This type of design matrix only allows the modelling of first-order response surfaces attributed to their levels for each independent input factor. It requires 3–5 levels of independent input factor for optimisation purposes, which can only be achieved using a three-level full factorial model. The three-level full factorial design number of experimental trials can be calculated by Eq. (17).

$$N = 2^k \tag{17}$$

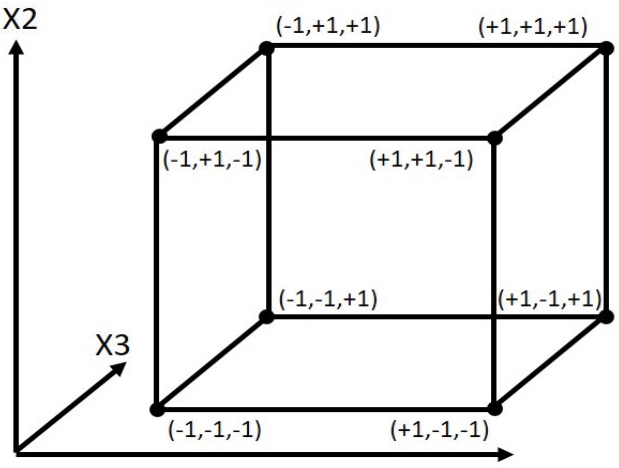

Fig. 10. Illustration of two-level full factorial design matrix with three independent inputs [48].

Nonetheless, the three-level full factorial design often relies on many experiments required compared with CCD and BBD designs, which in return makes it most costly to be run. Recently, it has been observed that the full factorial approach is widely applied in medical research, such as in [49,55]. However, it is less common in membrane science, where full factorial design is often used as a screening design to select the most important input factors and discard the less significant factors [55]. Nevertheless, despite their rare application in the membrane science field, recent research by Ebadi et al. [61] has successfully implemented the full factorial design to optimise the DCMD operational conditions at Esfahan Oil Refining Company (EORC) in Iran, as specified in Section 3.3.

Subsequently, Table 2 specifies and summarises each model of the experiment trials formula and factor levels that best suit each model. Hence, based on the three models portrayed in the review, the comparison for the number of experiments with different factors is further tabulated in Table 3. The three-level full factorial design results in a higher number of experiments that need to be run for an optimisation to be conducted compared with the central composite and Box–Behnken model. The central composite design, which requires more experiments than BBD, is due

to the repetitions of centre points applied in the design of experiment limits. Despite its lower number of experiments, the BBD design needs to be conducted with a factor less than 4, which is an advantage for this model; however, it was eliminated when runs with more than 4.

Table 2
Summary for models experiments trials formula and level of factors

Design of experiments	Experiments	Level	Factors [48]
Full factorial (2-Level)	$N = 2^k$	2	$2 < k < 5$
Full factorial (3-Level)	$N = 3^k$	3	$2 < k$
Box–Behnken	$N = 2(k(k-1)) + C$	3	$3 < k < 5$
Central composite	$N = k^2 + 2k + C_p$	5	$2k < 5$

3.4. Correlations between RSM-based model with mass and heat transfer model

As discussed in the section before, the mass and heat transfer model includes various parameters in the DCMD process, including membrane properties such as tortuosity and membrane pores. With various factors included in the mass and heat transfer model, the researcher may encounter problems in which factors to be studied for optimisation purposes. The independent factors for a study, on the other hand, are commonly chosen based on evaluating the most significant operational factor [56]. Table 4 summarises

Table 3
Comparison for central composite design, Box–Behnken design, and three-level full factorial design number of experiments for the optimisation process

Number of Factors	Central composite design	Box–Behnken design	Full factorial design (3-Level)
2	13 (5 Centre point repetition)	–	9
3	20 (6 Centre point repetition)	15	27
4	30 (6 Centre point repetition)	27	81
5	52 (full factorial)	46	243

Table 4
Common studied factors for optimisation of DCMD system

Reference	Membrane configuration	Input	Response
[57]	DCMD	Feed inlet temperature (40°C–80°C)	Average permeate flux
		Permeate inlet temperature (15°C–35°C)	Water productivity per unit volume of module
		Flow velocity of feed solution (6–54 m/min)	Water production per unit energy consumption
		Module packing density (5%–45%)	Comprehensive index
		Length-diameter ratio of module (3.3–16.7)	
[58]	DCMD	Initial feed concentration (30–25 wt.%)	Feed concentration increase
		Feed inlet temperature (65°C–55°C)	Transmembrane water flux
		Distillate inlet temperature (30°C–20°C)	
		Feed and distillate flow rates (1–0.4 L/min)	
[15]	DCMD	Feed temperature (50°C–80°C)	Permeate flux
		Permeate temperature (20°C)	Heat transfer rate
		Feed and distillate flowrate (0.2–0.8 LPM)	Temperature and concentration polarisation effect
		Pore Size (0.1–0.4 μM)	Temperature profile and energy efficiency
[66]	DCMD	Feed temperature (295–332.5 K)	Mass flux
		Feed flowrate (1.75–3.8 m/s)	
		Feed concentration (10–90 g/L)	
		Membrane thickness (0–350 μm)	
		Porosity (–15%–15%)	
[49]	DCMD	Flowrate of feed solution (0.4–0.9 L/min)	Water flux
		Flowrate of draw solution (0.3–0.7 L/min)	Salt reverse flux
		Concentration of draw solution (3–5 M)	
[14]	DCMD	Stirring rate (786.8–150 RPM)	Permeate flux
		Feed inlet temperature (50°C–22.3°C)	
		Feed concentration (2.193–0.2 M)	

factors that are commonly studied for the optimisation of DCMD in recent years. The most studied input parameters were found to be feed and permeate inlet temperatures, feed inlet concentration, and feed and permeate flowrate. Meanwhile, it is uncommon to find factors involving membrane properties, for example, pore size, membrane thickness and module packing density.

The DCMD process is heavily reliant on water vapour pressure as the driving force, emphasising the significance of increasing feed temperature in terms of improving flux permeation in the DCMD system [57,58]. Hence, for an efficient DCMD process, the temperature differential between the feed and permeates sides must be as large as possible within the system limit in order to aid in higher flux [59]. The significance of the feed temperature is also portrayed in the literature [60,61]. Furthermore, as demonstrated in previous studies [62,63], feed flowrate can affect DCMD performance by lowering the temperature and concentration polarisation on the membrane surface. Under ideal conditions, increasing the feed flowrate simultaneously increases the thermal efficiency, thus resulting in a rise in flux.

In contrast to the RO process, feed concentration is an interesting parameter in the case of a DCMD system due to its suitability for high salinity water treatment. On the other hand, the effect of the feed temperature and flowrate contribute more to the DCMD process as demonstrated in the previous study [61]. Membrane properties have been shown to increase permeate flux by increasing pore size and porosity while decreasing pore tortuosity and membrane thickness [64,65].

4. Current application of design matrix in modelling DCMD system

4.1. Box–Behnken design

Guillen-Burrieza et al. [56] demonstrated the use of BBD to optimise or model the DCMD system under various operating conditions in order to understand the operational parameter effects on the wetting phenomena [56]. In their study, the BBD model proposed 22 experiments to model the system. The research group highlights that the BBD design was used because it has fewer design points and thus takes less time to conduct the experiments. Four operational parameters were included: feed and permeate flowrates, permeate flux, wetting rate, and time when wetting was detected. The BBD model used in the study assumes a linear relationship between factors and response, with the results demonstrating a high R-value (0.953). Besides that, the results included a structural analysis to show which factors had a significant impact on the response itself. They discovered that the temperature of the feed and permeate were more important than the flow rate of the permeate. On the other hand, lower feed and permeate temperatures result in early wetting.

The Box–Behnken design matrix was used in a study by Zhou et al. [49] to study the forward osmosis–membrane distillation (FO–MD) process. The study also adopted RSM in optimising the FO–MD process. Feed flow rate, permeate flow rate, and permeate solution concentration were included as independent variables in modelling the system. The response includes maximising water flux and pollutants removal efficiency, and minimising salt reverse flux. The BBD was used to design three-factor and three-level experiments, resulting in a total of 17 experiments to be carried out. Meanwhile, under optimal conditions, the regression coefficient obtained for the system feed temperature is 0.9875, indicating a great correlation between the regression equation and the deviation data in the study and is significant to the MD process, as shown in Fig. 11.

4.2. Central composite design

The central composite design is one of the most popular approaches in modelling membrane distillation systems, mainly due to its suitability to caters for more than two factors while still providing high accuracy in optimisation results. In a study by Hubaidillah et al. [63]; a central

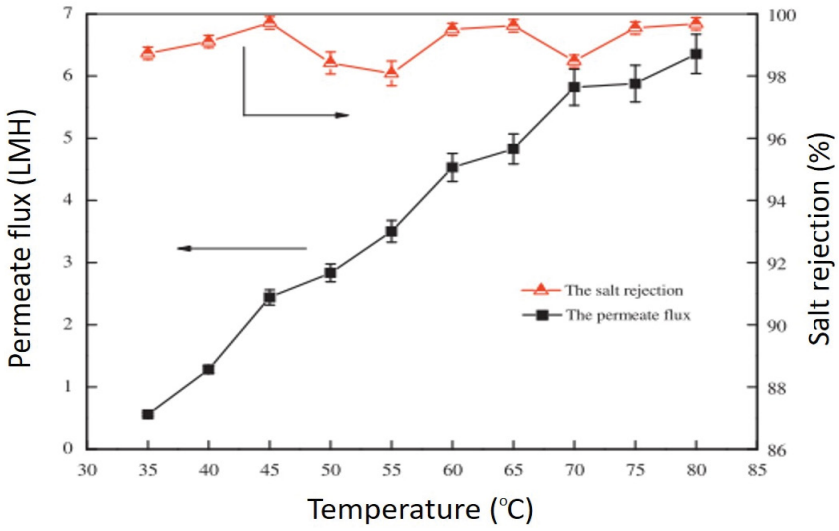

Fig. 11. Permeate flux and salt rejection with changes in inlet feed temperature and constant flow rate on both inlets [49].

composite design of the experiment was applied to model and optimise the DCMD system, using a cost-effective, green ceramic hollow fiber membrane for desalination. This green ceramic hollow fiber membrane was made from rice husk waste, making membrane production more cost-effective. The study optimised feed temperature, permeate temperature and feed flowrate as inputs, and permeate flux as a response [63]. To optimise the green membrane's DCMD process, 32 experiments and 3 replicate points were performed using central composite design as DOE. From the ANOVA results obtained by the CCD model, the feed flow rate is highly significant compared with the feed temperature, as shown in Fig. 12a. Meanwhile, Fig. 12b demonstrates that the permeate temperature and the feed flowrate did not have a significant effect of salt rejection.

Meanwhile, Abdelkader et al. [64] optimised the DCMD desalination process by investigating temperature difference, feed velocity, salt concentration and glucose concentration with permeate flux as a response. Both input and the response were modelled by 5 levels of central composite design. The simulated model demonstrated a high degree of correlation between the predicted and experimental values. According to the author, the model's R level is 0.967, indicating that it can explain 96.7% of data deviation. From the ANOVA results, the temperature difference and feed velocity have the most significant effect on the DCMD response. Meanwhile, the salt concentration appears to have a less significant positive effect on the permeate flux response, as shown in Fig. 13. This is due to the fact that increasing the feed flowrate and velocity decreases the differential temperature between the two sides of the membrane. Consequently, this condition has an effect on the feed stream viscosity and, as a result, increases the permeate flux.

4.3. Full factorial design

In a study by Ebadi et al. [61], the full factorial design was applied to optimise the desalination process at Esfahan Oil Refining Company (EORC), as shown in Fig. 14. The process involved using DCMD to implement polytetrafluoroethylene (PTFE) membrane for the rejected stream of RO system. The optimisation involved three-level factorials in the DOE. The optimisation focused mainly on DCMD operating parameter such as feed temperature, feed flow rate and permeate temperature, with permeate flux as the system corresponding response. Here, 32 sets of tests were proposed by the Design Expert Software. From the surface plot and regression equation, the author concludes that the permeate flux increased with increasing feed temperature and feed flowrate, and decreasing permeate temperature.

Rashid et al. [49] used the full factorial design matrix in their study for optimising the PVDF-co-HFP hollow fiber membrane with a 15-cm effective length for the DCMD system. The study introduced four operating parameters: feed temperature, feed flow rate, feed concentration, and polyvinylpyrrolidone (PVP) content. The study used second-order

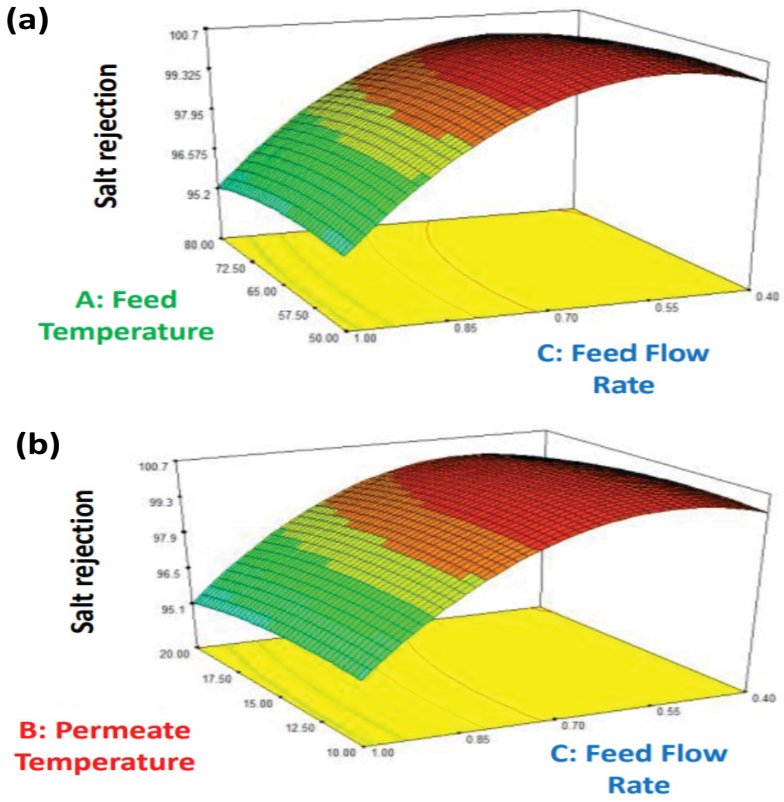

Fig. 12. Three-dimensional (3D) response surface plot of salt rejection as a function of operating factors: (a) feed temperature vs. feed flow rate and (b) permeate temperature vs. feed flow rate [61].

full factorial design matrix, which resulted in 16 times of experimentation. From the optimisation results, the significance level is PVP dope > feed temperature > feed flowrate > feed concentration, with a coefficient of determination (R^2) of 97.56%, indicating that the model depicted 97.56% of the data deviation. Fig. 15 depicts the surface plot from their study, which shows that flux increases with increasing feed temperature but nearly reaches a plateau with increasing feed flowrate.

5. Optimisation accuracy and most suitable model for optimisation of DCMD

Table 4 summarises the optimisation conditions for each study based on the current modelling application in the DCMD system in Section 3.0. By comparing the optimisation using the CCD design matrix (Table 5), it can be seen that as the number of experimental runs increases, with 3 to 4 independent variables, the deviation between the

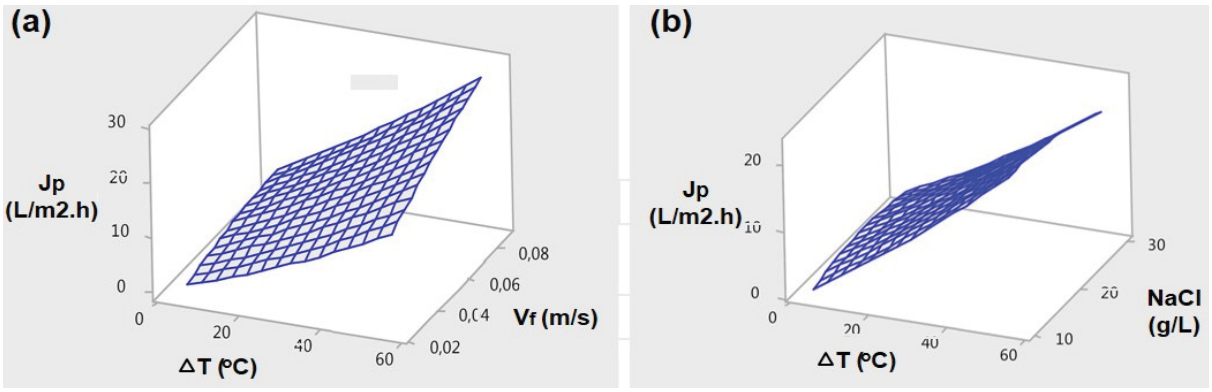

Fig. 13. Response surface plots as a function of (a) temperature difference vs. feed flowrate and (b) temperature difference vs. NaCl concentration [62].

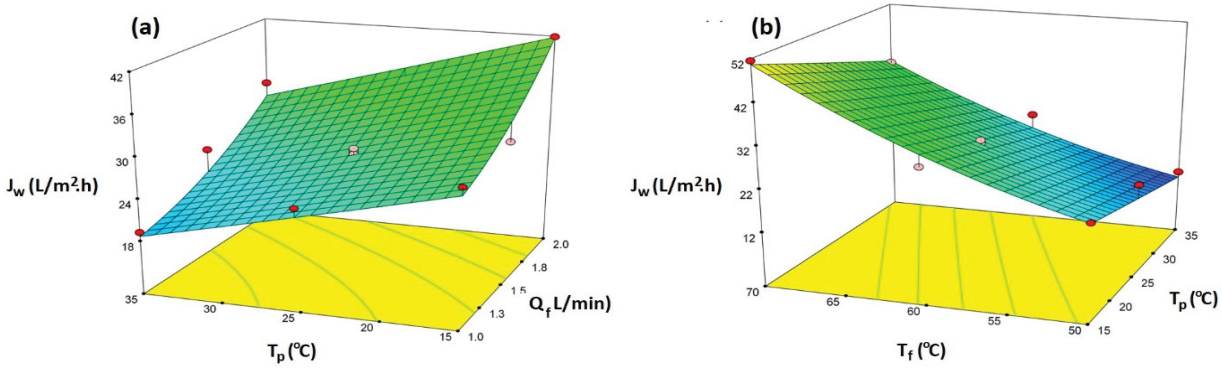

Fig. 14. (a and b) Graphical illustration of variable interactions for the proposed DCMD desalination at EORC refinery [61].

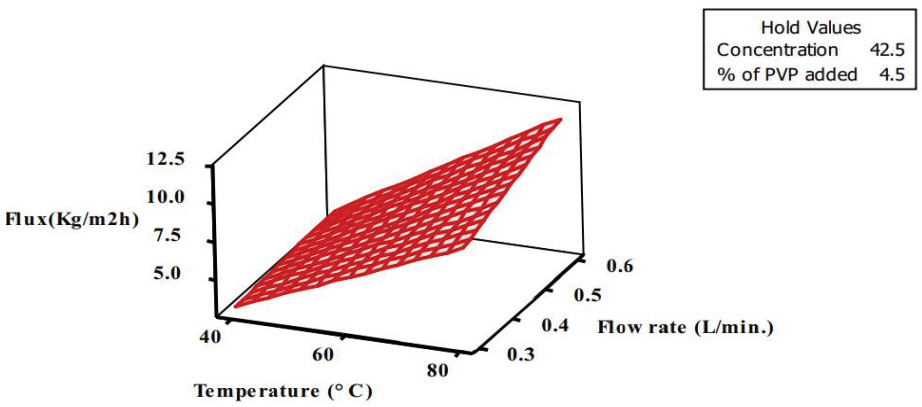

Fig. 15. Three-dimensional (3D) response surface plot of the expected permeate flux as a function of feed temperature and feed flow rate at constant fed concentration and PVP added [60].

Table 5
Input parameter and corresponding response

Design of experiment	Run times (simulation)	Factor						Response	Membrane area	% Deviation from exp. value	References
		Feed temperature (°C)	Permeate temperature (°C)	Temperature different (feed and permeate) (°C)	Feed flowrate	Distillate flowrate	Feed concentration	Permeate flux			
Full factorial	32	70	15	–	2 L/min	–	–	60.76 L/m^2 h	80 cm^2	3.5%	[61]
Full factorial	16	80	–	–	0.6 L/min	–	35 g/L	21 kg/m^2 h	Eff. Length 15 cm	–	[60]
Central composite design	32	70.15	19.84	–	0.58 L/min	–	–	35 kg/m^2 h	7.54 cm^2	0.5%	[63]
Central composite design	28	–	–	55.23	0.086 m/s	–	10.08 g/L	34.1 L/m^2 h	32 cm^2	4.3%	[62]
Central composite design	17	65	20.8	–	0.278 L/min	–	25 wt.%	2.94 kg/m^2 h	138 cm^2	2.8%	[58]
Box–Behnken design	20	60	30	–	30 L/h	–	–	26.5 L/m^2 h	30 cm^2	–	[56]
Box–Behnken design	17	72.5	–	–	0.87 L/min	0.31 L/min	4.82 M	4.65 L/m^2 h	21 cm^2	Near to experiment value	[45]

simulation value and the real experiment value decreases. On the other hand, it can be observed that for the same experiment run times, which is 32 for both CCD and full factorial design, and the same amount of input factor, the full factorial design has a higher percentage deviation from the experiments, with 3.5%, compared with 0.5% for the CCD design. This condition is attributed to the CCD design implementation, which used 5 levels per factor for modelling, while the full factorial design used three-level per factor.

Moreover, for the same DOE method, CCD, with the same number of input factors [59,63], slight differences in the number of experiments run resulted in a higher deviation from the experimental value. The CCC design and CCF design matrix application is identified with 5 levels and 3 levels per factor, respectively [62,58]. Even with 5 level implementations, the CCC design matrix produces a higher deviation than the CCF design. The nature of CCC design which includes the generation of new extremes for each input that is outside of the range, explains the deviation of the optimisation from the CCF design. The BBD model, which has the fewest experimental runs, still achieved a comparable experimental value for its optimisation. However, due to the lack of recent implementation of the BBD model for the DCMD system, its optimisation suitability by RSM cannot be fully concluded in this review and requires further research.

From all of the models discussed in this paper, the majority of the models, BBD, full factorial, and CCD, provide nearly the same range of deviation 0%–5% from the experimental condition. In comparison with the full factorial model, the CCD model is recommended for an input factor of 3. It can be observed that the temperature and flowrate of feed and permeate are mainly investigated to model the DCMD system. Meanwhile, other operating parameters such as the membrane area and DMCD configuration, among others, should also be taken into consideration to generate optimum condition.

6. Conclusion and future directions

Membrane distillation has gained an increasing amount of interest over the year, whether it's for modelling, applications or testing parameters. The MD technologies are suitable for removal of different contaminants such as heavy metals, organics and inorganic salt. The fundamentals of DCMD were briefly discussed in this review, as well as models used to optimise operating conditions in the system. This review identified the most important parameters that most researchers have focused on in recent years: feed temperature, velocity, and concentration all of which can affect the efficiency of the DCMD process. Although multiple parameters play an important role in the DCMD process, conventional optimisation still falls short of correlating the impact/significance of the parameters to each other. In contrast, optimisation using response surface methodology has recently been implemented in a study. With proper design matrix selection, its deviation from the experimental value is minimal.

A proper selection of design matrix may require implementing screening method using the 2-level factorial method, before proceeding with optimisation of the identified parameter. The CCD model was the most commonly used for DCMD, with the researchers specifying a range of 3–4 independent input variables. In comparison to the full factorial model and the BBD, the CCD model with the highest number of experiments has the lowest deviation when a similar range of input is used. However, for a BBD model, future studies must be conducted to validate its suitability for the DCMD process, as there is a lack of study that specifically outlines its optimisation deviation from experimentation value, in which it cannot be concluded clearly in this review.

The level of each DOE implements in studying the DCMD system is important in obtaining the optimum results. Designs that may include the generation of new extremes values necessitate further investigation by researchers. Finally, with technological advancements increasing the efficiency of the DCMD process by the day, optimisation study may need to focus on commercial application to overcome the limitations of these optimisation techniques that commonly subjected to lab-scale applications. Other than CCD, BBD, and FFD, there are many other models that may be suitable for the optimisation process that are not mentioned in this review.

Acknowledgement

The authors gratefully acknowledge the Malaysia Ministry of Higher Education (MOHE) for the FRGS research funding provided (600-IRMI/FRGS 5/3 (441/2019)).

References

[1] N.S. Fuzil, N.H. Othman, N.H. Alias, F. Marpani, M.H.D. Othman, A.F. Ismail, W.J. Lau, K. Li, T.D. Kusworo, I. Ichinose, M.M.A. Shirazi, A review on photothermal material and its usage in the development of photothermal membrane for sustainable clean water production, Desalination, 517 (2021) 115259, doi: 10.1016/j.desal.2021.115259.

[2] A.M. Karam, T.M. Laleg-Kirati, Membrane fouling modeling and detection in direct contact membrane distillation, J. Process Control., 81 (2019) 190–196, doi: 10.1016/j.jprocont.2019.05.013.

[3] J. Ravi, M.H.D. Othman, T. Matsuura, M. Ro'il Bilad, T.H. El-badawy, F. Aziz, A.F. Ismail, M.A. Rahman, J. Jaafar, Polymeric membranes for desalination using membrane distillation: a review, Desalination, 490 (2020) 114530, doi: 10.1016/j.desal.2020.114530.

[4] M. Al-Salmi, M. Laqbaqbi, S. Al-Obaidani, R.S. Al-Maamari, M. Khayet, M. Al-Abri, Application of membrane distillation for the treatment of oil field produced water, Desalination, 494 (2020) 114678, doi: 10.1016/j.desal.2020.114678.

[5] S. Ali, S.A.U. Rehman, H.Y. Luan, M.U. Farid, H. Huang, Challenges and opportunities in functional carbon nanotubes for membrane-based water treatment and desalination, Sci. Total Environ., 646 (2019) 1126–1139.

[6] R. Castro-Muñoz, Breakthroughs on tailoring pervaporation membranes for water desalination: a review, Water Res., 187 (2020) 116428, doi: 10.1016/j.watres.2020.116428.

[7] G. Guan, H. Lou, C. Yao, J. Li, X. Yang, Achieving sustainable operation for hypersaline membrane distillation applications: a novel strategy based on the critical Reynolds number, Desalination, 499 (2021) 114833, doi: 10.1016/j.desal.2020.114833.

[8] Z.S. Tai, M.H.D. Othman, A. Mustafa, J. Ravi, K.C. Wong, K.N. Koo, S.K. Hubadillah, M.A. Azali, N.H. Alias, B.C. Ng, M.I.H. Mohamed Dzahir, A.F. Ismail, M.A. Rahman, J. Jaafar, Development of hydrophobic polymethylhydrosiloxane/tetraethylorthosilicate (PMHS/TEOS) hybrid coating on ceramic membrane for desalination via membrane distillation, J. Membr. Sci., 637 (2021) 119609, doi: 10.1016/j.memsci.2021.119609.

[9] F.E. Ahmed, R. Hashaikeh, N. Hilal, Hybrid technologies: the future of energy efficient desalination–a review, Desalination, 495 (2020) 114659, doi: 10.1016/j.desal.2020.114659.
[10] J. Lou, J. Vanneste, S.C. DeCaluwe, T.Y. Cath, N. Tilton, Computational fluid dynamics simulations of polarization phenomena in direct contact membrane distillation, J. Membr. Sci., 591 (2019) 117150, doi: 10.1016/j.memsci.2019.05.074.
[11] Y.M. Manawi, M. Khraisheh, A.K. Fard, F. Benyahia, S. Adham, Effect of operational parameters on distillate flux in direct contact membrane distillation (DCMD): comparison between experimental and model predicted performance, Desalination, 336 (2014) 110–120.
[12] C. Liu, L. Chen, L. Zhu, Fouling mechanism of hydrophobic polytetrafluoroethylene (PTFE) membrane by differently charged organics during direct contact membrane distillation (DCMD) process: an especial interest in the feed properties, J. Membr. Sci., 548 (2018) 125–135.
[13] W. Jantaporn, A. Ali, P. Aimar, Specific energy requirement of direct contact membrane distillation, Chem. Eng. Res. Des., 128 (2017) 15–26.
[14] M. Khayet, C. Cojocaru, C. García-Payo, Application of response surface methodology and experimental design in direct contact membrane distillation, Ind. Eng. Chem. Res., 46 (2007) 5673–5685.
[15] S. Noamani, S. Niroomand, M. Rastgar, A. McDonald, M. Sadrzadeh, Development of a self-sustained model to predict the performance of direct contact membrane distillation, Sep. Purif. Technol., 263 (2021) 118407, doi: 10.1016/j.seppur.2021.118407.
[16] M. Laqbaqbi, M.C. García-Payo, M. Khayet, J. El Kharraz, M. Chaouch, Application of direct contact membrane distillation for textile wastewater treatment and fouling study, Sep. Purif. Technol., 209 (2019) 815–825.
[17] M.S. Ismail, A.M. Mohamed, D. Poggio, M. Pourkashanian, Direct contact membrane distillation: a sensitivity analysis and an outlook on membrane effective thermal conductivity, J. Membr. Sci., 624 (2021) 119035, doi: 10.1016/j.memsci.2020.119035.
[18] I. Hitsov, T. Maere, K. De Sitter, C. Dotremont, I. Nopens, Modelling approaches in membrane distillation: a critical review, Sep. Purif. Technol., 142 (2015) 48–64.
[19] A. Boubakri, A. Hafiane, S.A.T. Bouguecha, Application of response surface methodology for modeling and optimization of membrane distillation desalination process, J. Ind. Eng. Chem., 20 (2014) 3163–3169.
[20] H.Y. Wu, M. Tay, R.W. Field, Novel method for the design and assessment of direct contact membrane distillation modules, J. Membr. Sci., 513 (2016) 260–269.
[21] L. Song, B. Li, K.K. Sirkar, J.L. Gilron, Direct contact membrane distillation-based desalination: novel membranes, devices, larger-scale studies, and a model, Ind. Eng. Chem. Res., 46 (2007) 2307–2323.
[22] Y. Dong, X. Dai, L. Zhao, L. Gao, Z. Xie, J. Zhang, Review of transport phenomena and popular modelling approaches in membrane distillation, Membranes, 11 (2021) 1–27.
[23] E. Ali, Dynamic analysis and modeling of direct contact membrane distillation for water desalination during startup using linear system theory, Chem. Eng. Process. Process Intensif., 136 (2019) 17–27.
[24] D.J. Park, E. Norouzi, C. Park, Experimentally-validated computational simulation of direct contact membrane distillation performance, J. Heat Mass Transfer, 129 (2019) 1031–1042.
[25] A. Bamasag, T. Alqahtani, S. Sinha, N. Ghaffour, P. Phelan, Experimental investigation of a solar-heated direct contact membrane distillation system using evacuated tube collectors, Desalination, 487 (2020) 114497, doi: 10.1016/j.desal.2020.114497.
[26] J.G. Lee, W.S. Kim, J.S. Choi, N. Ghaffour, Y.D. Kim, Dynamic solar-powered multi-stage direct contact membrane distillation system: concept design, modeling and simulation, Desalination, 435 (2018) 278–292.
[27] M.I. Soomro, W.S. Kim, Performance and economic evaluation of linear Fresnel reflector plant integrated direct contact membrane distillation system, Renewable Energy, 129 (2018) 561–569.
[28] R. Baghel, S. Upadhyaya, S.P. Chaurasia, K. Singh, S. Kalla, Optimization of process variables by the application of response surface methodology for naphthol blue black dye removal in vacuum membrane distillation, J. Cleaner Prod., 199 (2018) 900–915.
[29] K.S.S. Christie, T. Horseman, S. Lin, Energy efficiency of membrane distillation: simplified analysis, heat recovery, and the use of waste-heat, Environ. Int., 138 (2020) 105588, doi: 10.1016/j.envint.2020.105588.
[30] Z. Yan, H. Yang, F. Qu, H. Yu, H. Liang, G. Li, J. Ma, Reverse osmosis brine treatment using direct contact membrane distillation: effects of feed temperature and velocity, Desalination, 423 (2017) 149–156.
[31] S. Soukane, M.W. Naceur, L. Francis, A. Alsaadi, N. Ghaffour, Effect of feed flow pattern on the distribution of permeate fluxes in desalination by direct contact membrane distillation, Desalination, 418 (2017) 43–59.
[32] M. Pagliero, M. Khayet, C. García-Payo, L. García-Fernández, Hollow fibre polymeric membranes for desalination by membrane distillation technology: a review of different morphological structures and key strategic improvements, Desalination, 516 (2021) 115235, doi: 10.1016/j.desal.2021.115235.
[33] Q.L. Ve, R. Koirala, M. Bawahab, H. Faqeha, M.C. Do, Q.L. Nguyen, A. Date, A. Akbarzadeh, Experimental investigation of the effect of the spacer and operating conditions on mass transfer in direct contact membrane distillation, Desalination, 500 (2021) 114839, doi: 10.1016/j.desal.2020.114839.
[34] B. Li, Y. Yun, M. Wang, C. Li, W. Yang, J. Li, G. Liu, Superhydrophobic polymer membrane coated by mineralized β-FeOOH nanorods for direct contact membrane distillation, Desalination, 500 (2021) 114889, doi: 10.1016/j.desal.2020.114889.
[35] K. Marques Lisboa, D. Busson de Moraes, C. Palma Naveira-Cotta, R. Machado Cotta, Analysis of the membrane effects on the energy efficiency of water desalination in a direct contact membrane distillation (DCMD) system with heat recovery, Appl. Thermal Eng., 182 (2021) 116063, doi: 10.1016/j.applthermaleng.2020.116063.
[36] A.S. Niknejad, S. Bazgir, A. Sadeghzadeh, M.M.A. Shirazi, Evaluation of a novel and highly hydrophobic acrylonitrile-butadiene-styrene membrane for direct contact membrane distillation: electroblowing/air-assisted electrospraying techniques, Desalination, 500 (2021) 114893, doi: 10.1016/j.desal.2020.114893.
[37] A. Khalifa, A. Mezghani, H. Alawami, Analysis of integrated membrane distillation-heat pump system for water desalination, Desalination, 510 (2021) 115087, doi: 10.1016/j.desal.2021.115087.
[38] F. Eleiwi, N. Ghaffour, A.S. Alsaadi, L. Francis, T.M. Laleg-Kirati, Dynamic modeling and experimental validation for direct contact membrane distillation (DCMD) process, Desalination, 384 (2016) 1–11, doi: 10.1016/j.desal.2016.01.004.
[39] Z. Kuang, R. Long, Z. Liu, W. Liu, Analysis of temperature and concentration polarizations for performance improvement in direct contact membrane distillation, J. Heat Mass Transfer., 145 (2019) 118724, doi: 10.1016/j.ijheatmasstransfer.2019.118724.
[40] N. Dutta, B. Singh, S. Subbiah, P. Muthukumar, Performance analysis of a single and multi-staged direct contact membrane distillation module integrated with heat recovery units, Chem. Eng. J. Adv., 4 (2020) 100055, doi: 10.1016/j.ceja.2020.100055.
[41] J. Zhang, S. Gray, J. De Li, Predicting the influence of operating conditions on DCMD flux and thermal efficiency for incompressible and compressible membrane systems, Desalination, 323 (2013) 142–149.
[42] R.D. Gustafson, J.R. Murphy, A. Achilli, A stepwise model of direct contact membrane distillation for application to large-scale systems: experimental results and model predictions, Desalination, 378 (2016) 14–27.
[43] J.D. Gil, A. Ruiz-Aguirre, L. Roca, G. Zaragoza, M. Berenguel, Prediction models to analyse the performance of a commercial-scale membrane distillation unit for desalting brines from RO plants, Desalination, 445 (2018) 15–28.

[44] M. Yolmeh, S.M. Jafari, Applications of response surface methodology in the food industry processes, Food Bioprocess Technol., 10 (2019) 413–433.
[45] Y. Zhou, M. Huang, Q. Deng, T. Cai, Combination and performance of forward osmosis and membrane distillation (FO-MD) for treatment of high salinity landfill leachate, Desalination, 420 (2017) 99–105.
[46] A. Ruiz-Aguirre, J.A. Andrés-Mañas, J.M. Fernández-Sevilla, G. Zaragoza, Modeling and optimization of a commercial permeate gap spiral wound membrane distillation module for seawater desalination, Desalination, 419 (2017) 160–168.
[47] S. Bhattacharya, Central Composite Design for Response Surface Methodology and Its Application in Pharmacy, P. Kayaroganam, Ed., Response Surface Methodology in Engineering Science, IntechOpen, doi: 10.5772/intechopen.95835. Available at: https://www.intechopen.com/chapters/74955
[48] I.M. Fukuda, C.F.F. Pinto, C.D.S. Moreira, A.M. Saviano, F.R. Lourenço, Design of experiments (DoE) applied to pharmaceutical and analytical quality by design (QbD), Braz. J. Pharm. Sci., 54 (2018) 1–16.
[49] Y. Zhou, M. Huang, Q. Deng, T. Cai, Combination and performance of forward osmosis and membrane distillation (FO-MD) for treatment of high salinity landfill leachate, Desalination, 420 (2017) 99–105.
[50] J.S. Rao, B. Kumar, 3D Blade Root Shape Optimization, Woodhead Publishing Limited, 2012. doi: 10.1533/9780857094537.4.173.
[51] B. Ait-Amir, P. Pougnet, A. El Hami, Meta-model development, Embedded Mechatronic Systems, 2 (2015) 151–179.
[52] D. Ozturk, E. Dagdas, B.A. Fil, M.J.K. Bashir, Central composite modeling for electrochemical degradation of paint manufacturing plant wastewater: one-step/two-response optimization, Environ. Technol. Innovation, 21 (2021) 101264, doi: 10.1016/j.eti.2020.101264.
[53] D. Ozturk, T. Sahan, T. Bayram, A. Erkus, Application of response surface methodology (RSM) to optimize the adsorption conditions of cationic Basic Yellow 2 onto pumice samples as a new adsorbent, Fresenius Environ. Bull., 26 (2017) 3285–3292.
[54] M. Mathur, V. Kusumdevi, Design of experiment : a novel and systematic approach of developing formulations in pharmaceuticals, World J. Pharm. Res., 8 (2019) 865–877.
[55] P. Yazgan-Birgi, M.I. Hassan Ali, H.A. Arafat, Comparative performance assessment of flat sheet and hollow fiber DCMD processes using CFD modeling, Sep. Purif. Technol., 212 (2019) 709–722.
[56] E. Guillen-Burrieza, M.O. Mavukkandy, M.R. Bilad, H.A. Arafat, Understanding wetting phenomena in membrane distillation and how operational parameters can affect it, J. Membr. Sci., 515 (2016) 163–174.
[57] D. Cheng, W. Gong, N. Li, Response surface modeling and optimization of direct contact membrane distillation for water desalination, Desalination, 394 (2016) 108–122.
[58] J. Liu, H. Ren, F.I. Hai, A.K. Albdoor, Z. Ma, Direct contact membrane distillation for liquid desiccant regeneration and fresh water production: experimental investigation, response surface modeling and optimization, Appl. Therm. Eng., 184 (2021) 116293, doi: 10.1016/j.applthermaleng.2020.116293.
[59] M.R. Elmarghany, A.H. El-Shazly, M.S. Salem, M.N. Sabry, N. Nady, Thermal analysis evaluation of direct contact membrane distillation system, Case Stud. Therm. Eng., 13 (2019) 100377, doi: 10.1016/j.csite.2018.100377.
[60] K.T. Rashid, S.B.A. Rahman, Q.F. Alsalhy, Optimum operating parameters for hollow fiber membranes in direct contact membrane distillation, Arabian J. Sci. Eng., 41 (2016) 2647–2658.
[61] M. Ebadi, M.R. Mozdianfard, M. Aliabadi, Employing full factorial design and response surface methodology for optimizing direct contact membrane distillation operational conditions in desalinating the rejected stream of a reverse osmosis unit at Esfahan refinery–Iran, Water Sci. Technol. Water Supply, 19 (2019) 492–501.
[62] S. Abdelkader, A. Boubakri, S.U. Geissen, L. Bousselmi, Direct contact membrane distillation applied to saline wastewater: parameter optimization, Water Sci. Technol., 77 (2018) 2823–2833.
[63] S.K. Hubadillah, M.H. Dzarfan Othman, P. Gani, A.F. Ismail, M.A. Rahman, J. Jaafar, A green membrane distillation system for seawater desalination: response surface modelling and optimization, IOP Conf. Ser.: Mater. Sci. Eng. 361 (2018) 1–5, doi: 10.1088/1757-899X/361/1/012011.
[64] E. Drioli, A. Ali, F. Macedonio, Membrane distillation: recent developments and perspectives, Desalination, 356 (2015) 56–84.
[65] R. Ullah, M. Khraisheh, R.J. Esteves, J.T. McLeskey, M. AlGhouti, M. Gad-el-Hak, H. Vahedi Tafreshi, Energy efficiency of direct contact membrane distillation, Desalination, 433 (2018) 56–67.
[66] A. Bahmanyar, M. Asghari, N. Khoobi, Numerical simulation and theoretical study on simultaneously effects of operating parameters in direct contact membrane distillation, Chem. Eng. Process. Process Intensif., 61 (2012) 42–50.